

**MEMS accelerometers and distributed sensing for rapid earthquake
characterization**

Jesse F. Lawrence^{1*}

Elizabeth S. Cochran²

Angela Chung¹

Anna Kaiser³

Carl M. Christensen¹

Richard Allen⁴

Jack W. Baker¹

Bill Fry³

Thomas Heaton⁵

Deborah Kilb⁶

Monica D. Kohler⁵

Michela Tafer⁷

*To whom correspondence should be made (jflawrence@stanford.edu)

¹Stanford University, USA

²University of California, Riverside, USA

³GNS Science, New Zealand

⁴University of California, Berkeley, USA

⁵California Institute of Technology, USA

⁶University of California, San Diego, USA

⁷University of Delaware, USA

Introductory Paragraph:

Earthquake early warning efforts aim to detect earthquakes and provide seconds of warning for surrounding populations. Here, we test the feasibility of rapidly detecting and characterizing earthquakes with the Quake-Catcher Network (QCN), which connects low-cost MicroElectromechanical Systems (MEMS) accelerometers to a volunteer network of Internet-connected computers. We benchmark QCN's real-time detections against GNS Science's GeoNet earthquake detections for the aftershock sequence of the 3 September 2010 M_w 7.2 Darfield, New Zealand earthquake. Under normal network operations, QCN detected and characterized earthquakes within 9.1 seconds of the earthquake rupture and determined the magnitude within 1 magnitude unit for 90% of the detections.

Rapid detection and characterization of earthquakes can provide nearby populations with seconds of earthquake early warning (EEW) prior to strong shaking¹. Regional EEW systems have been proposed, tested, or implemented

in relatively few regions, including California²⁻⁴, Japan^{1,5}, Mexico^{6,7}, Taiwan⁸, and Turkey⁹. Rapid earthquake detection is primarily limited by the high costs of instrumentation and required infrastructure. Japan has the most developed EEW system, with over 1000 traditional seismic stations spaced at ~20 km intervals¹. The Japanese system recently issued a successful alert during the 11 March, 2011 M_w 9 Tōhoku, Japan earthquake¹⁰.

EEW systems rapidly determine the location and magnitude of an ongoing earthquake rupture. Earthquake locations are estimated from the arrival times of seismic waves propagating across a sensor network. While peak ground velocity (PGV) or acceleration (PGA) can be used to estimate earthquake magnitude^{11,12}, the scatter in PGV and PGA requires measurements from multiple stations to yield stable earthquake magnitude estimates¹³. Thus earthquake magnitude estimates are often delayed by seconds to minutes in regions with fewer seismic sensors or slow data communications. Because most regions have sparse seismic networks, more sophisticated data analyses are required to obtain stable estimates with fewer measurements. For example, *various* algorithms^{3,5} analyze the period of the *P*-wave velocity or displacement, which provides an earthquake magnitude estimate. To use this method with accelerometer data, accelerograms must be integrated once or twice to velocity or displacement, which can be less reliable at higher-noise sites like those in urban areas. Here, we describe the real-time detection algorithm implemented for the Quake-Catcher Network. This

algorithm monitors peak acceleration (as a three-component vector magnitude) between 0 and 4 seconds following the onset of new strong motions detected at each sensor-station, $PGA_{i,a}0-4$ (additional information on nomenclature in Supplementary Material S1).

New sensor technology and computational techniques provide an avenue for reducing the cost of building dense seismic networks and implementing EEW systems. Small and low-cost MicroElectroMechanical Systems (MEMS) triaxial sensors yield high quality records of ground acceleration¹⁴⁻¹⁸. Utilizing the public's computing resources through the Berkeley Open Infrastructure for Network Computing (BOINC) volunteer computing infrastructure^{19,20}, we minimize the costs associated with monitoring sensors¹⁴⁻¹⁶. By attaching MEMS accelerometers to Internet-connected volunteer computers, the Quake-Catcher Network (QCN) has successfully recorded hundreds of earthquakes (M_w 2.6 to M_w 8.8) around the world²¹.

Following the 3 September 2010 M_w 7.2 Darfield, New Zealand earthquake²², QCN and GNS Science installed 192 14-bit MEMS accelerometers in the Christchurch region (Fig. 1). All 192 sensors were installed on volunteer computers in homes and businesses within 11 days of the mainshock, monitoring the rich aftershock sequence. See^{14-16,21} for details on sampling rate (50Hz), timing errors ($< \pm 20$ ms), and more.

The low-cost QCN MEMS accelerometers and traditional GeoNet accelerometers, operated by GNS Science, provide similar accelerations, velocities, and displacements for sensors that are close to each other²⁴. As shown in Figure 2, both networks show similar scatter in PGA (PGA is calculated for the whole waveform following the *P* wave) due to source, path, and site effects. This suggests that for moderate to large earthquakes at close distances, lower resolution QCN sensors installed in noisy environments (homes and offices) provide reliable PGA measurements.

On 25 September 2010, QCN implemented preliminary real-time earthquake detection and characterization by exploiting trigger information from the dense QCN network in Christchurch. At each QCN sensor, strong ground shaking is automatically detected when the acceleration within a short-term window is significantly higher than the long-term average acceleration²⁴. At the time of a strong new acceleration, the volunteer computer transmits a digital data package (a “trigger”) to the QCN server. Trigger information includes time, peak vector amplitude of acceleration, $\max(|a|)$, at the time of the trigger, t_0 , ($\text{PGA}_{|a|0}$), and station information. Triggers transfer rapidly from the volunteer computer to the server (2-5 seconds)¹⁵, which is critical for EEW (additional information in Supplementary Material S2).

Triggers are temporally and spatially correlated by QCN's server to evaluate association with a regional earthquake rather than isolated, single-station noise. We evaluate triggers received at 0.2-second intervals, comparing each trigger with all other triggers that occurred within the previous 100 seconds. If triggers occur within 100 seconds and the stations are located within 200 km they are considered "roughly correlated"¹⁴. Once the number of roughly correlated triggers exceeds an empirical regional threshold (6-7 stations in New Zealand), we then locate the earthquake by a three-dimensional grid search for the earthquake hypocenter¹⁴; Supplemental Figure S3²¹.

Then QCN estimates the earthquake magnitude, a critical measurement for EEW. Earthquake magnitude is often estimated by fitting the peak ground acceleration (PGA) as a function of distance^{11,12,25}. The scatter in PGA is often quite high due to regionally heterogeneous geologic material and site conditions at each sensor [e.g. Fig. 2;¹³]. However, PGA measured at multiple stations can provide a stable magnitude estimate. For New Zealand, we obtain the empirical relationship between magnitude, distance, and $PGA_{|a|}$:

$$M = 0.03\Delta + 1.09 \ln(PGA_{|a|}) + 4.28$$

where Δ is distance in km and $PGA_{|a|}$ is the vector sum of the three-component PGA in m/s^2 . This relationship is similar to those reported for New Zealand crustal earthquakes by Zhao *et al.*²⁵, McVerry *et al.*,²⁶ and Campbell and

Bozorgnia²⁷ and suggests that previously determined PGA-distance-magnitude relationships can be used (More details available in Supplementary Material S4).

QCN host computers transmit updated $PGA_{|a|}$ measurements at $t = 1, 2,$ and 4 seconds after the initial trigger ($PGA_{|a|1-4}$), which are used to improve magnitude estimates. New data between iterations may consist of: 1) new triggers ($PGA_{|a|0}$) reported by additional sensors or from new wave arrivals from the same sensor, and 2) the $PGA_{|a|1-4}$ updates. The number of iterations for an earthquake depends on the earthquake location and magnitude relative to the distribution of seismic stations.

Between 25 September and 1 April 2011 the QCN sensors detected 116 earthquakes ranging in size from M_l 3.6 – M_l 6.3 (Figs. 1 and 3). The minimum and median detection times were 3.1 and 9.8 seconds after the estimated earthquake origin time (Fig. 3a). This time includes: 1) source-to-sensor propagation time (varies); 2) trigger detection (fraction of a second); 3) transfer of trigger information to QCN's server (2-5 seconds); 4) trigger association and event declaration (requires at least 5 associated triggers, varies); and 5) earthquake location and magnitude estimation (< 0.5 second). The median magnitude estimate increases by 0.5 magnitude units during the first four iterations, likely due to the fact that smaller earthquakes often result in only one

or two iterations; larger events typically yield more iterations because more sensors trigger with equal or greater PGA_{lat} 0-4.

To determine the accuracy of QCN's real-time detection and characterization we compare the QCN earthquake catalog with the published GNS Science catalog²⁸. With the exception of the period within 2 days of the 21 February 2011 M6.3 Christchurch earthquake (see Supplemental material S5), QCN automatically detected all earthquakes M5 or larger and all except four GNS-reported M4.5 or larger earthquakes that occurred within 15km of the array. Importantly, after an initial algorithm adjustment period (see Supplemental material S5), QCN produced no false-positive earthquake detections.

Figure 3 compares the origin time, location, and magnitude for the QCN and GeoNet seismic networks. QCN's rapid earthquake detections compare favorably to the GNS Science catalog. On average, we find that the median error in earthquake location is ~7 km, the QCN earthquake origin times are biased 1.5 seconds early, and the magnitude estimates are ~0.5 magnitude units too high. These differences can be attributed to two factors: network distribution and velocity and attenuation models. The QCN sensors are clustered in a small region (10×10 km²) with the majority of the earthquakes occurring outside of the network (Fig. 1). This tends to increase the location error, biasing earthquake

locations farther from the network, and leading to over-estimation of magnitude and earlier origin times (Fig. 3).

QCN automatically generates an AlertMap (Fig. 4) (2) for each detected earthquake, which illustrates estimated peak ground shaking intensities and the estimated time until shaking arrives at each location. Here, intensity is estimated as instrumental intensity^{28,29}, using $PGA_{\text{Iai}0-4}$ instead of PGA. The smooth background contour of shaking intensity provides an interpolated estimate of the ground shaking, which is useful for determining which sub-regions to notify of incoming significant ground motion¹. The individual $PGA_{\text{Iai}0-4}$ observations at each sensor delineate fine-scale variability in ground shake intensity useful for emergency response teams, who need immediate spatial information before power and data communications may fail. QCN successfully disseminated automated real-time EEW alerts to a small test population of QCN personnel based on input parameters such as earthquake v. alert recipient location and magnitude or intensity (see Supplemental Information S5). These EEW alerts, including AlertMaps content, were received in a fraction of a second of detection and characterization.

Given the high quality of results observed in this study, further analysis will benefit from attempting more sophisticated techniques. While the use of $PGA_{\text{Iai}0-4}$ was largely successful in for this experiment, it is known that near field PGA

can saturate whereas other measurements such as the maximum period of displacement³ can be more reliable². Dense networks such as described above provide a unique opportunity to test a variety of EEW algorithms^{2,4}.

In conclusion, this rapid deployment illustrates the potential for low-cost seismic networks to contribute vital information for use in earthquake early warning. The Quake-Catcher Network is designed for low-overhead installation of dense strong-motion seismic networks capable of near real-time earthquake detection and characterization. With the planned installation of >6000 higher-resolution USB MEMS accelerometers over the next three years, QCN will be able to generate real-time EEW data products for moderate to large mainshock earthquakes in many more earthquake-prone regions. This expansion will be particularly beneficial for populations that cannot afford to support a traditional seismic network for EEW data products. Furthermore, integration with regional seismic networks will further improve earthquake detection and characterization for existing or developing EEW systems. The expansion of scientific EEW data products resulting from this type of low-cost seismic network is likely to continue; however, the more complex socio-political issues of when and how to alert the populations remain.

Figures:

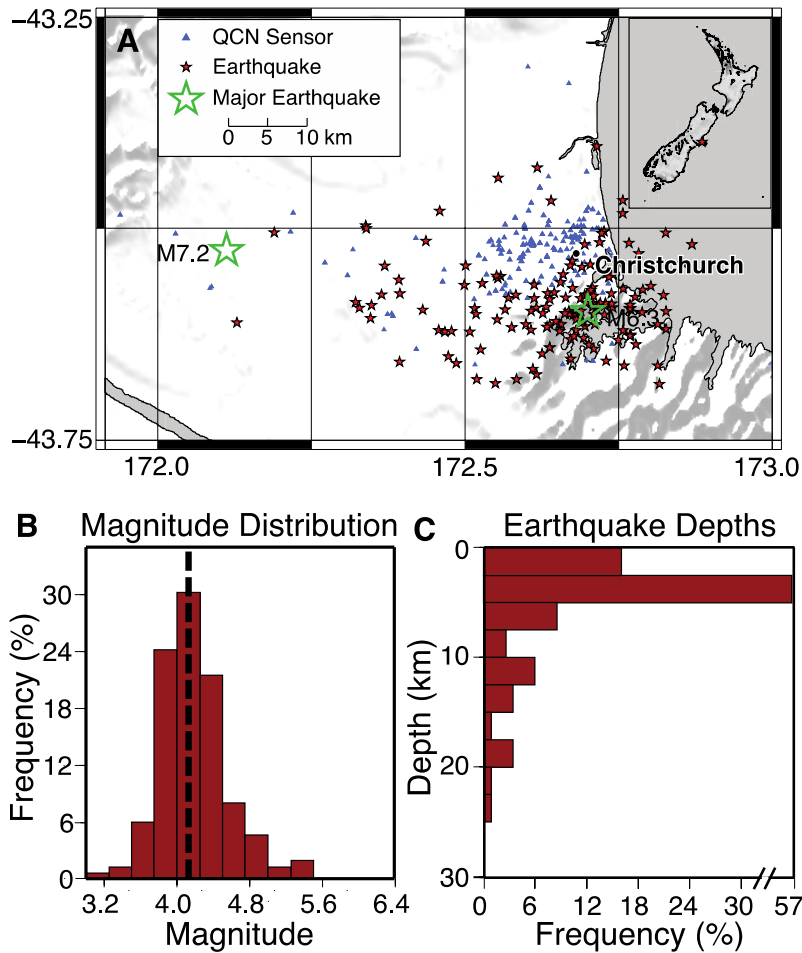


Figure 1. Seismic sensors and earthquakes detected by QCN's rapid earthquake detection between 25 September 2010 and 1 April 2011. (A) Map of QCN sensors (blue triangles), detected earthquakes (red stars), and major earthquakes (green stars). Inset map shows the study area (red star); (B) magnitude distribution; and (C) depth distribution of detected earthquakes.

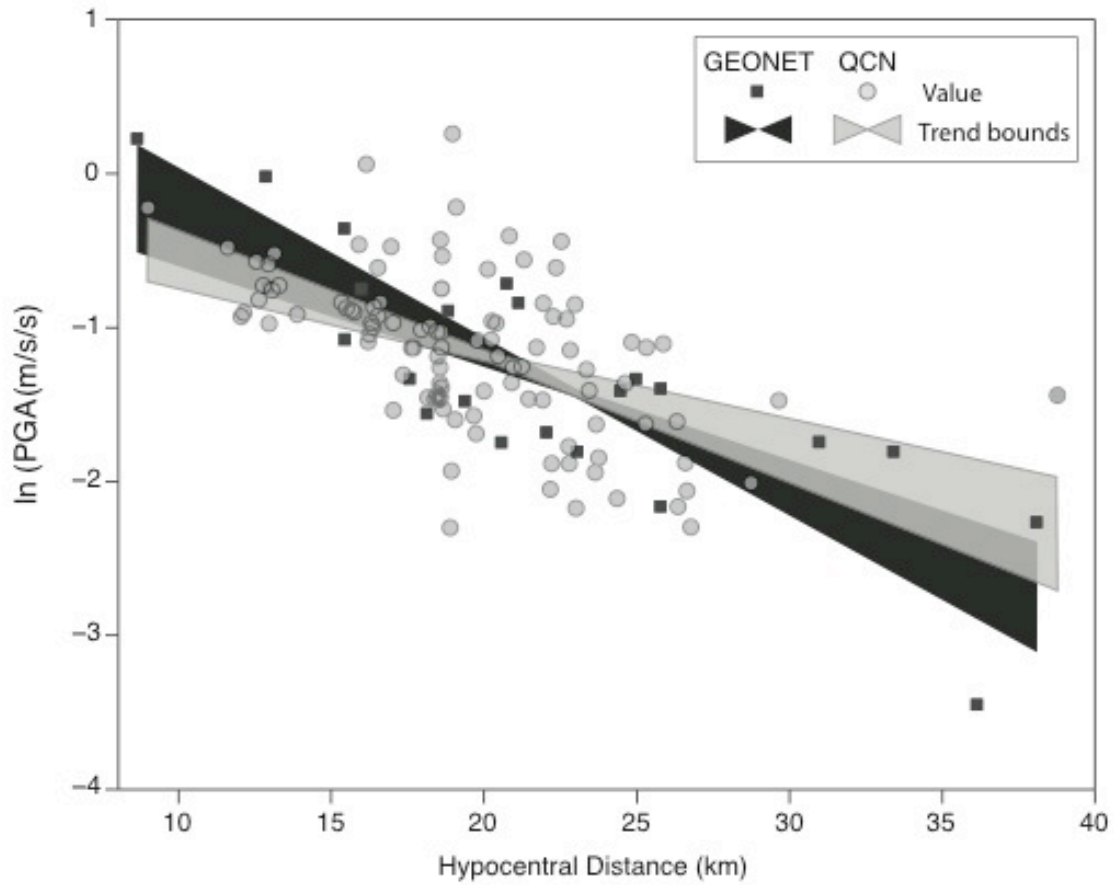


Figure 2. Comparison of $PGA_{|a|}$ versus hypocentral distance for a 15 October 2010 M4.7 earthquake observed by QCN (grey circles) and GeoNet (black squares) sensors. The data were fit by linear regression and trend bounds (grey and black shading) were determined by bootstrap resampling.

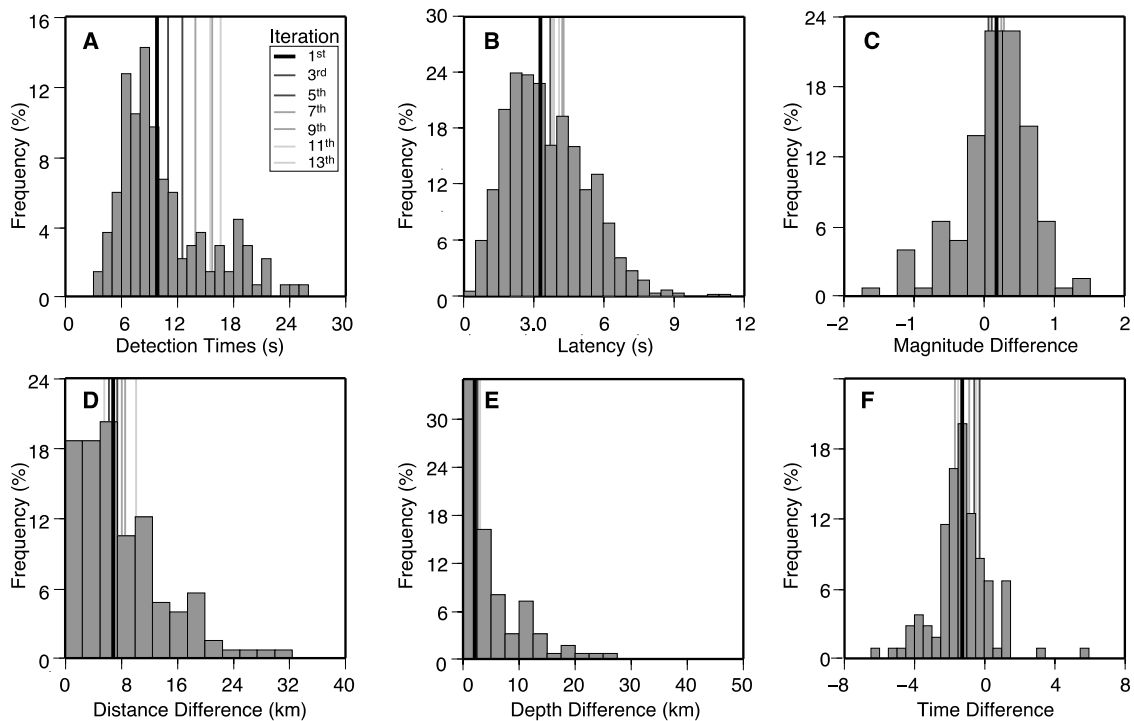
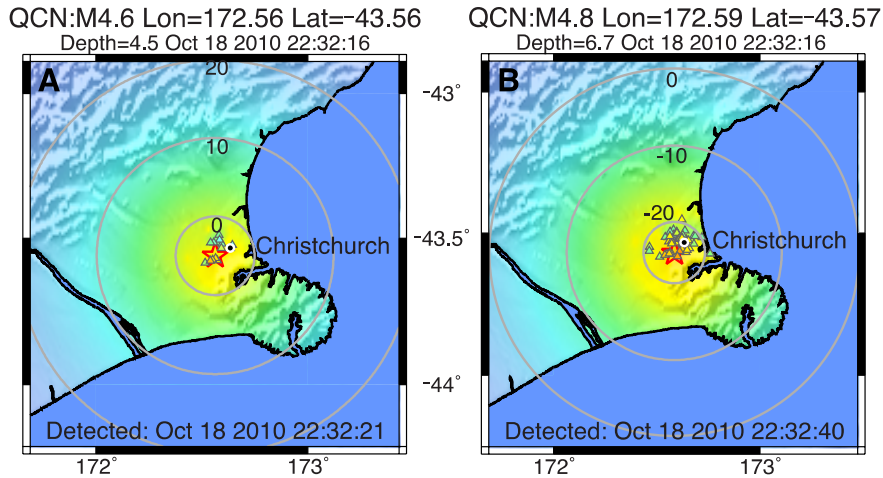


Figure 3: Rapid earthquake detection statistics for 116 earthquake detections between 25 September 2011 to 1 April 2011. (A) Time from the estimated earthquake origin to the initial earthquake detection. (B) Latency from host signal detection to trigger registry on the QCN server. Distribution comparing QCN rapid earthquake characterization and GNS catalog of: (C) Magnitude; (D) Epicentral location; (E) Depth; and (F) Origin time (sec). Histograms are for the first iteration; lines indicate median values for each iteration. The magnitudes are within 0.5 and 1.0 magnitude units for 63% and 90% of all earthquakes, respectively.



Perceived Shaking	Not felt	Weak	Light	Moderate	Strong	Very strong	Severe	Violent	Extreme
Potential Damage	none	none	none	Very light	Light	Moderate	Moderate/Heavy	Heavy	Very Heavy
Peak Acc. (%g)	<0.17	0.17-1.4	1.4-4.0	4.0-9	9-17	17-32	32-61	61-114	>114
Peak Vel. (cm/s)	<0.12	0.12-1.1	1.1-3.4	3.4-8	8-16	16-31	31-59	59-115	>115
Instrumental Intensity	I	II-III	IV	V	VI	VII	VIII	IX	X+

Figure 4. AlertMaps generated (A) 5 s and (B) 24 s after the earthquake origin time by QCN's rapid earthquake detection system for a M4.8 Christchurch earthquake. The grey circles illustrate isochrons for S-wave arrival time relative to the detection time (positive times indicate expected future arrivals, negative times indicate waves have arrived)². The early AlertMaps are very similar to the later iterations. The intensity scale is from^{29,30}.

Supplementary Material:

S1: A Note on PGA Nomenclature

This manuscript describes peak ground accelerations in a variety of instances that may differ from traditional measurements. The traditional peak ground acceleration (PGA), which includes the full waveform, is not useful for earthquake early warning because it requires recording the entire waveform before making a measurement. Therefore, we introduce a variant of peak-ground acceleration up to time lag, τ : PGA_{τ} . Time lag, τ , is relative to time of detecting a strong new motion. Such detections are usually performed with some form of short-term average to long-term average ratio, STA/LTA²⁴. The peak acceleration at the time of the trigger, $\tau=0$, is given by PGA_0 . The peak acceleration up to 4 seconds following trigger is denoted by PGA_4 .

This paper also examines the maximum vector magnitude of the acceleration, $|a|$, rather than dividing the horizontal or vertical magnitudes separately. Note that we de-mean each component prior to taking the magnitude of the vector. The peak vector magnitude of acceleration $PGA_{|a|}$ is typically dominated by the peak horizontal acceleration, PGA_H . Note that $PGA_{|a|}$ removes on the partitioning of energy between vertical and horizontal, which may vary due to site conditions,

source mechanism, and earth structure. In some cases within this paper we refer to $PGA_{|a|}$ and in other cases we refer to $PGA_{|a|\tau}$. The peak vector magnitude accelerations at the time of the trigger and up to 4 seconds following the trigger are given by $PGA_{|a|0}$ and $PGA_{|a|4}$. It should be noted that near the source, PGA and $PGA_{|a|4}$ are typically very similar.

S2: Trigger Latency

There is a finite time delay between the time of initial short-term/long-term average detection on the volunteer computer and the time the associated trigger is registered in QCN's database. This latency accrues as the trigger and data up to the trigger time are first saved to the volunteer computer, the xml trigger information is uploaded to QCN's server, and the server parses and registers the trigger information. Fig. S2 illustrates the probability and cumulative distribution functions for the trigger latencies of sensors in California and worldwide. The mean latencies are ~ 3.4 and 4.2 s for California and worldwide respectively and over 90% of all triggers are registered within 6 and 7 seconds for California and worldwide, respectively. There are several factors that may contribute to lower latency within California: 1) proximity to the server in California; 2) faster average Internet connections in California; or 3) faster computers in California. If the lower latency is due to proximity (i.e. fewer Internet connections), then adding QCN servers in earthquake-prone regions around the world could further reduce latencies.

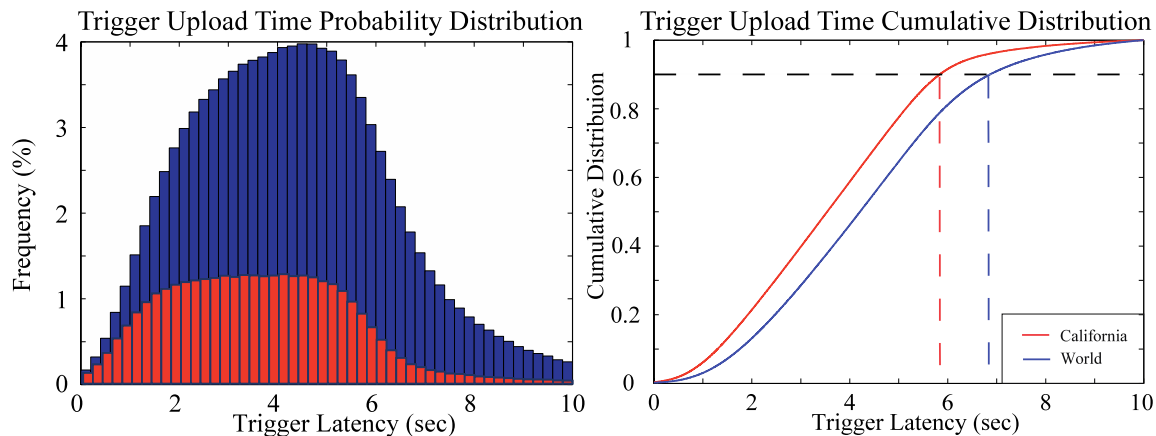


Figure S2. Latency (sec) for trigger information detected on a volunteer computer to be transferred to the QCN central server located in California. (Left) Histogram and (Right) cumulative distribution of trigger latencies. Distributions in blue indicate latencies from all QCN stations distributed globally and red distributions are latencies for stations in California.

S3. Hypocenter Determination

Details of the earthquake location algorithm are available in¹⁴. Figure S3 shows the correlation between the estimated travel times and the observed travel times for the 21 February 2011 M6.3 earthquake. On average, QCN observes hypocenters within ~7km of the GNS reported locations, which have reported errors on the order of 1km in latitude and longitude. Differences in estimated hypocenter may result from the greater level of noise in the QCN data, the use of different location algorithms, and different biases resulting from employing different *a priori* seismic velocity models. The excellent correlation (e.g., Fig. S3,

where $R^2 > 0.94$) between observed and theoretical travel times for the best-fit source locations suggests well located events, given the *a priori* seismic velocity model.

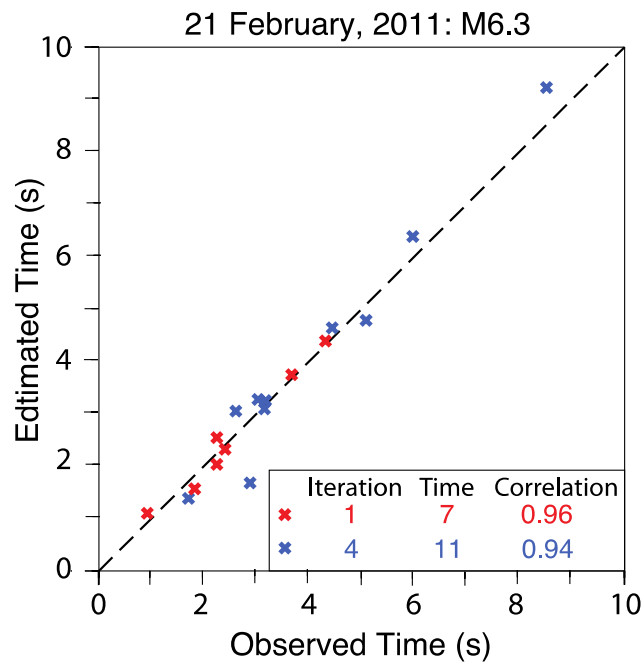


Figure S3: Correlation of modeled travel times to observed travel times for the M6.3 earthquake on 21 February 2011, with values shown for detection iteration 1 (red) and 4 (blue). A similar online accessible²¹ figure is automatically generated for each iteration based on the best-fit location determined by a 3D grid search. This correlation between observed and estimated travel times are used in the rapid earthquake location scheme. Only models with correlations better than $R^2 > 0.5$ are considered “probable earthquakes”.

S4: Magnitude-Distance-PGA Relationship

We compare the magnitude-distance-PGA relationship used in the QCN rapid event detection to those previously reported by Zhao *et al.* ²⁵, McVerry *et al.*, ²⁶ and Campbell and Bozorgnia, ²⁷. Note, this is a traditional full waveform PGA discussed here. There is significant variation in the published relationships and the one determined in our work, which is due to wide scatter in measured accelerations due to source and site effects (Fig. S4). Note that the models of Zhao *et al.*, ²⁵, McVerry *et al.*, ²⁶ and Campbell and Bozorgnia, ²⁷ are intended for earthquakes with magnitudes greater than M5, which may also account for some misfit to the data.

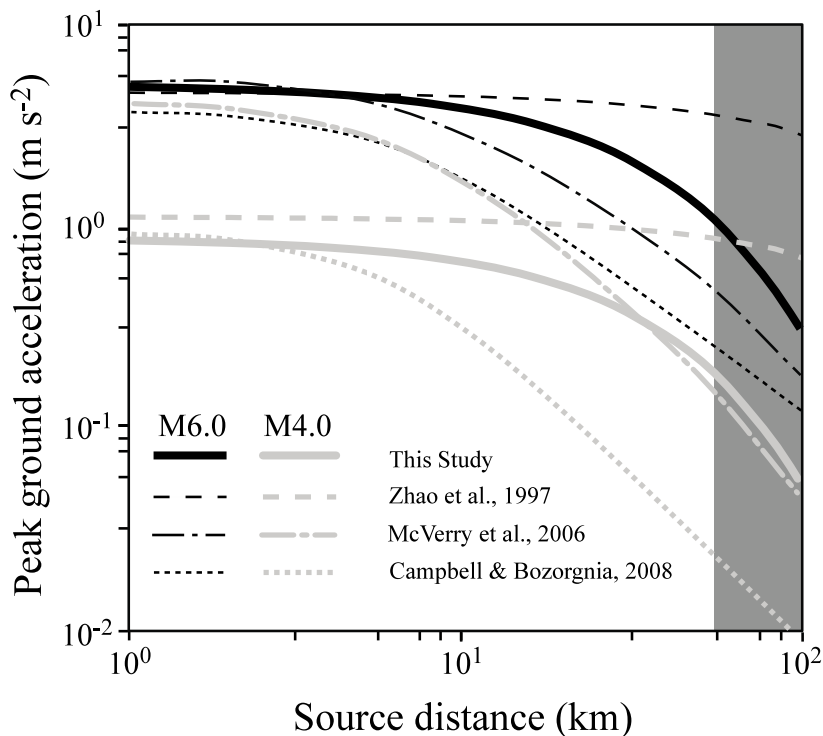


Figure S4. Comparison between the PGA relationship obtained here and the relationship of Zhao *et al.*, ²⁵, McVerry *et al.*, ²⁶ and Campbell and Bozorgnia, ²⁷.

Note the relationships deviate more at greater distances; however, there are fewer QCN PGA measurements available to constrain the relationship at the larger distances (grey region).

S5: Timeline of Real-Time Implementation

We implemented QCN's real-time rapid earthquake detection earlier than anticipated when we activated the rapid aftershock mobilization program (RAMP) in New Zealand following the 3 September 2010 M7.2 Darfield earthquake. We had completed retrospective testing of the earthquake detection algorithms for data recorded during a RAMP following the M8.8 Maule Chile earthquake¹⁴. Our primary goal in this RAMP deployment was to record earthquakes with a very dense network, but also to test the real-time detection algorithms. We implemented a preliminary version of the detection algorithms on 25 September 2011 and, over the following months, added features, improved algorithms, and expanded the real-time output features.

Due to the relatively high noise level of the sensors, many (~51) earthquakes with magnitude greater than M3.5 were not automatically detected within 15 km of the array shown in Fig. 1, as expected. Waveform records of these missed detections were uploaded to QCN's server so delayed characterization was possible in most cases, with detections possible for earthquakes as small as $M_I=2.6$. During the first 32 days, 11 false positive earthquakes were erroneously

detected and characterized, usually with a low number (5-6) of triggering stations. After several algorithm improvements implemented in October 2010, no false detections and characterizations have been reported. The most important algorithm change was to not analyze triggers from sensors that repetitively trigger due to chronic computer malfunction or extremely high noise.

The network size reduced gradually throughout the deployment period (11 September 2010 – 1 April 2011) as we only requested volunteer participation for ~6 weeks during the early aftershock period following the 3 September 2011 M7.2 Darfield earthquake. Immediately prior to the 21 February 2011 M6.3 Christchurch earthquake, only 40 ± 10 sensors were operating in the region. GNS re-deployed sensors south of Christchurch following the M6.3 Christchurch earthquake, bringing the network back up to 50 ± 10 sensors. As expected, the network capabilities diminish as the number of sensors decreased. Nevertheless, dozens of earthquakes were detected and recorded prior to the M6.3 earthquake when fewer sensors were reporting.

Following the 21 February 2011 M6.3 Christchurch earthquake the capabilities of the real time detection were further reduced due to the following: 1) power outages; 2) rapid succession of aftershocks; and 3) lower numbers of sensors in the region. Vigorous aftershock sequences typically challenge even the most expensive and robust EEW systems^{31,32}. QCN failed to detect 54 aftershocks

with magnitude greater than M3.5 in the 48 hours following the M6.3 Christchurch earthquake. With ongoing and planned algorithm changes aimed at discriminating between event updates and new events, we expect fewer complications for future vigorous aftershock sequences.

S6: EEW Dissemination

Dissemination of alert messages is the final step of EEW. While the technical logistics have largely been overcome (e.g., JMA^{1,10}), dissemination of an alert is typically the purview of local government agencies due to liability concerns. We therefore side-step the complex socio-political questions of when and how alerts might be disseminated. Instead, this manuscript primarily focuses on the feasibility of rapid earthquake detection and characterization. Nevertheless, we conducted a basic test to determine if QCN is capable of automatically issuing rapid alerts. The initial test of this alert system was conducted in-house and no alerts were provided to the general public.

Beginning 5 March 2011, QCN has automatically determined a list of potential recipients to whom EEW alerts should be generated for each detected event. The alerts can be filtered by the distance a recipient is from the source as well as by a participant-defined magnitude threshold. The alert, sent via e-mail, includes the earthquake metadata (origin time, location, and magnitude) and an AlertMap. This information is sent to recipients, typically within 1 second, using

Simple Mail Transfer Protocol (SMTP) and Internet Message Access Protocol (IMAP). SMTP and IMAP are not ideal for immediate mass data dissemination, but the rudimentary test illustrated that earthquake information detected by the low-cost QCN network could be distributed rapidly.

References:

- 1 Hoshiba, M., O. Kamigaichi, M. Saito, S. Tsukada, and N. Hamada, . Earthquake Early Warning Starts Nationwide in Japan, . *EOS* **89**, 73-80 (2008).
- 2 Allen, R. M. *et al.* Real-time earthquake detection and hazard assessment by ElarmS across California. *Geophys. Res. Lett.* **36**, doi:doi:10.1029/2008GL036766. (2009).
- 3 Allen, R. M. & Kanamori, H. The Potential for Earthquake Early Warning in Southern California. *Science* **300**, 786 (2003).
- 4 Cua, G. & Heaton, T. H. in *Earthquake Early Warning Systems.* (eds P. Gasparini, G. Manfredi, & J. Zschau) (Springer Berlin Heidelberg, 2007).
- 5 Nakamura, Y. in *Proc. World Conf. Earthquake Eng.* . 673.
- 6 Anderson, J., R. Quaas, S. K. Singh, J. M. Espinosa-Aranda, A. Jimenez,, J. Lermo, J. C., S. E Sanchez, R. Meli, M. Ordaz, S. Alcocer, & B. Lopez, L. A., E. Mena, and C. Javier The Copala Guerrero, Mexico earthquake of September 14, 1995 (MW - - 7.4): A preliminary report. *Seism. Res. Lett.* **66**, 11-19 (1995).
- 7 Espinosa-Aranda JM, J. A., Ibarrola G, & Alcantar F, A. A. Mexico City seismic alert system. *Seismol. Res. Lett.* **66**, 42–53 (1995).
- 8 Wu, Y. M. & Kanamori, H. Experiment on an onsite early warning method for the Taiwan earthquake information release system. *Seismol. Res. Lett.* **68**, 931–943 (2005).
- 9 Erdik, M. *et al.* Technical note: Istanbul earthquake rapid response and the early warning system. *Bulletin of Earthquake Engineering* **1**, 157-163 (2003).
- 10 JMA. *Japan Meteorological Agency: Earthquake Early Warning*, <www.jma.go.jp> (2011).
- 11 Donovan, N. C. in *Proc. 5th World Conf. Earthquake Engineering.* 1252-1261. (Edigraaf).
- 12 Gutenberg, B. & Richter, C. F. Earthquake magnitude, intensity, energy and acceleration. *Bull. Seism. Soc. Am.* **46**, 105-145 (1956).
- 13 Aoi, S., Kunugi, T. & Fujiwara, H. Trampoline Effect in Extreme Ground Motion. *Science.* **322**, 727-730 (2008).
- 14 Chung, A. *et al.* Catching quakes in Chile with a Rapid Aftershock Mobilization Program *Seismol. Res. Lett.*, in pres (2011).
- 15 Cochran, E., Lawrence, J. F., Christensen, C. & Chung, A. A Novel strong-motion seismic network for community participation in earthquake monitoring. *IEEE Instrumentation & Measurement Magazine* **12**, 8-15, doi:doi:10.1109/MIM2009.5338255 (2009).
- 16 Cochran, E. S., Lawrence, J. F., Christensen, C. & Jakka, R. S. The Quake-Catcher Network; citizen science expanding seismic horizons. *Seismological Research Letters* **80**, 26-30 (2009).
- 17 Farine, M., Thorburn, N. & Mougnot, D. General application of MEMS sensors for land seismic acquisition—is it time? *The Leading Edge* **23**, 246–250 (2004).

- 18 Holland, J. Earthquake data recorded by the MEMS accelerometer. *Seismological Research Letters* **74** (2003).
- 19 Anderson, D. P., and J. Kubiawicz. The world-wide computer. *Scientific American* **286**, 40–47 (2002).
- 20 Christensen, C., T. Aina, and D. Stainforth. in *First International Conference on e-Science and Grid Computing*, . 8–15 (Institute of Electrical and Electronics Engineers.).
- 21 QCN. *Information on the Quake-Catcher Network (QCN) earthquakes and earthquake sensing technologies can be found at <http://qcn.stanford.edu>*, (2011).
- 22 Gledhill, K. *et al.* The Darfield (Canterbury, New Zealand) Mw 7.1 Earthquake of September 2010: A Preliminary Seismological Report. *Seismological Research Letters* **82**, 378-386, doi:DOI: 10.1785/gssrl.82.3.378 (2010).
- 23 Cochran, E. S. *et al.* Comparison between low-cost and traditional MEMS accelerometers: A case study from the M7.1 Darfield, New Zealand aftershock deployment. *Annals of Geophysics (in review)* (2011).
- 24 Earle, P. S. & Shearer, P. M. Characterization of global seismograms using an automatic picking algorithm. *Bull. Seismol. Soc. Am.* **84**, 366-376 (1994).
- 25 Zhao, J. X., Dowrick, D. J. & McVerry, G. H. Attenuation of peak ground accelerations in New Zealand earthquakes. *Bulletin of the New Zealand National Society for Earthquake Engineering* **3**, 133-158 (1997).
- 26 McVerry, G. H., Zhao, J. X., Abrahamson, N. A. & Somerville, P. G. New Zealand acceleration response spectrum attenuation relations for crustal and subduction zone earthquakes. . *Bulletin of the New Zealand Society for Earthquake Engineering* **39**, 1-58 (2006).
- 27 Campbell, K. W. & Yousef Bozorgnia. NGA Ground Motion Model for the Geometric Mean Horizontal Component of PGA, PGV, PGD and 5% Damped Linear Elastic Response Spectra for Periods Ranging from 0.01 to 10s *Earthquake Spectra* **24**, 139-171 doi:doi:10.1193/1.2857546 (2008).
- 28 GNS-Science. 2011).
- 29 Wald, D. J., Quitoriano, J. V., Heaton, T. H., Kanamori, H. & Scriner, C. W. Relationship between Peak Ground Acceleration, Peak Ground Velocity, and Modified Mercalli Intensity for Earthquakes in California. *Earthquake Spectra* **15**, 537-555 (1999).
- 30 Wald, D. J. *et al.* TriNet "ShakeMaps": Rapid Generation of Peak Ground-motion and Intensity Maps for Earthquakes in Southern California. *Earthquake Spectra* **15**, 537-556 (1999).
- 31 Kanamori, H. in *Earthquake Early Warning Summit*.
- 32 Kilb, D., Martynov, V. G. & Vernon, F. L. Aftershock Detection Thresholds as a Function of Time: Results from the ANZA Seismic Network following the 31 October 2001 ML 5.1 Anza, California, Earthquake *Bull. Seism. Soc. Am.* **97**, 280-792, doi:doi: 10.1785/0120060116 (2007).
33. We thank the hundreds of QCN volunteer hosts and field crew, without whom this study would never have occurred. Many thanks to Dave Anderson whose support and augmentation of BOINC has allowed QCN

grow quickly into the world's largest and lowest-cost real-time seismic network. We thank Hiroo Kanamori and Dan McNamara for thorough feedback during the revisions of this manuscript. This research was supported in part by NSF EAR 1027802 and the New Zealand Natural Hazards Research Platform.